FEBS Letters

FEBS PRESS science publishing by scientists

The coordinated action of glucuronoyl esterase and α-glucuronidase promotes the disassembly of lignin–carbohydrate complexes

Olanrewaju Raji[1], Jenny Arnling Bååth[2,*], Thu V. Vuong[1], Johan Larsbrink[2], Lisbeth Olsson[2] and Emma R. Master[1,3]

1 Department of Chemical Engineering and Applied Science, University of Toronto, ON, Canada
2 Department of Biology and Biological Engineering, Wallenberg Wood Science Center, Chalmers University of Technology, Gothenburg, Sweden
3 Department of Bioproducts and Biosystems, Aalto University, Espoo, Finland

Correspondence
L. Olsson, Division of Industrial Biotechnology, Dept. of Biology and Biological Engineering, Chalmers University of Technology, kemivägen 10, SE-412 96 Gothenburg, Sweden
Tel: +46 31 772 3805
E-mail: lisbeth.olsson@chalmers.se

Present address
* Department of Biotechnology and Biomedicine, Technical University of Denmark, Søltofts Plads, Kgs. Lyngby, DK-2800, Denmark

(Received 14 October 2020, revised 24 November 2020, accepted 25 November 2020, available online 10 January 2021)

doi:10.1002/1873-3468.14019

Edited by Ulf-Ingo Flügge

Glucuronoxylans represent a significant fraction of woody biomass, and its decomposition is complicated by the presence of lignin–carbohydrate complexes (LCCs). Herein, LCCs from birchwood were used to investigate the potential coordinated action of a glucuronoyl esterase (*Tt*CE15A) and two α-glucuronidases (*Sde*Agu115A and *Axy*Agu115A). When supplementing α-glucuronidase with equimolar quantities of *Tt*CE15A, total MeGlc*p*A released after 72 h by *Sde*Agu115A and *Axy*Agu115A increased from 52% to 67%, and 61% to 95%, respectively. Based on the combined *Tt*CE15A and *Axy*Agu115A activities, ~ 34% of MeGlc*p*A in the extracted birchwood glucuronoxylan was occupied as LCCs. Notably, insoluble LCC fractions reduced soluble α-glucuronidase concentrations by up to 70%, whereas reduction in soluble *Tt*CE15A was less than 30%, indicating different tendencies to adsorb onto the LCC substrate.

Keywords: 4-*O*-methyl D-glucuronic acid; carbohydrate-active enzymes; enzyme adsorption; glucuronoxylan; hemicellulases; lignin–carbohydrate complexes

Hemicelluloses typically account for between 25% and 40% of plant cell walls and are characterized by β-(1→4)-linked carbohydrate backbones that can be substituted by additional monosaccharides and noncarbohydrate groups. In deciduous species, hemicelluloses are mainly represented by acetylated glucuronoxylan, which has a backbone comprised of β-(1→4)-linked xylopyranose (Xyl*p*) units, decorated with 4-*O*-methyl-D-glucuronic acid (MeGlc*p*A) at a reported frequency of 1 MeGlc*p*A for every 8–15 Xyl*p* [1,2], and acetyl units at C2 and/or C3 positions [3]. Coniferous species also contain xylans, in this case arabinoglucuronoxylans, where the β-(1 → 4)-linked Xyl*p* backbone is decorated with approximately 1 arabinofuranosyl (Ara*f*) and 2 MeGlc*p*A substitutions for every 14 Xyl*p* residues [4], though without acetylation of the backbone [5]. Detailed characterization of glucuronoxylan structures in *Arabidopsis thaliana* reveals an even patterning of MeGlc*p*A and acetate groups along the backbone, which is thought to facilitate xylan

Abbreviations
GH, glycoside hydrolase; HPAEC, high-performance anion-exchange chromatography; LCCs, lignin–carbohydrate complexes; PAD, pulsed amperometric detection.

association with the hydrophilic surface of cellulose [6–9] and outward orientation of MeGlc*p*A substitutions [10,11]. Arabinoglucuronoxylans from spruce (*Picea abies*) have been shown to display a combination of even patterned and clustered MeGlc*p*A and Ara*f* substitutions along the xylan backbone [12].

The diversity and recalcitrance of xylan structures are increased through the formation of covalent linkages to lignin. In deciduous and coniferous xylan sources, lignin–carbohydrate complexes (LCCs) include ester linkages between MeGlc*p*A substitutions of xylan and phenylpropane subunits in lignin [13–17]. For example, roughly 30% of the MeGlc*p*A residues in xylan from beechwood (*Fagus crenata*) [18,19] have been estimated to participate in ester-linked LCCs.

Given the complexity of xylan structures and their association with multiple plant cell wall components, several enzyme families are required for their full deconstruction [20]. So far, the combined action of xylan-active enzymes has mostly been studied to promote the complete conversion of xylans to fermentable sugars [21–23]. Enzymes predicted to act on LCCs, including α-glucuronidases (EC 3.2.1.131) belonging to glycoside hydrolase (GH) family GH115 (www.cazy.org) [24,25], and glucuronoyl esterases belonging to family CE15 [13,26–28], could facilitate xylan recovery and be used in higher-value applications [24,25,29,30].

Both bacterial and fungal GH115 α-glucuronidases have been characterized, and apart from *Bt*GH115A from *Bacteroides thetaiotaomicron*, which targets arabinogalactans [31], all characterized members preferentially release MeGlc*p*A substitutions in xylans ([23–25,31–37]; summarized in Table S1). GH115 enzymes with resolved structures or structure homology models are reported to adopt a four-domain architecture [31,32], except for *Sde*Agu115A from *Saccharophagus degradans* and *Axy*Agu115A from *Amphibacillus xylanus*, which adopt a five-domain architecture [24,25]. Despite their structural similarity, *Axy*Agu115A shows significantly higher activity at alkaline pH and comparatively high activity on complex xylans when compared to *Sde*Agu115A [25].

Most CE15 glucuronoyl esterases, including *Tt*CE15A from *Teredinibacter turnerae*, have been characterized using model substrates such as D-glucuronic acid benzyl ester, D-glucuronic acid allyl ester, D-glucuronic acid methyl ester, and D-galacturonic acid methyl ester [26,27,38,39]. It has also been confirmed that *Tt*CE15A does not exhibit significant acetyl esterase activity [38]. In a few cases, CE15 glucuronoyl esterases have been tested using LCC preparations. For example, Arnling Bååth *et al.* [13] reported a reduction in molecular weight and increase in carboxylic acid content of LCCs isolated from spruce and birch (*Betula pendula*) following treatment with the glucuronoyl esterase from *Acremonium alcalophilum* (*Aa*GE1). Similarly, the glucuronoyl esterase from *Cerrena unicolor* (*Cu*GE) releases uronic acid-containing xylooligosaccharides from extracted birchwood [40,41]. Furthermore, structural characterization of *Tt*CE15A, *Ot*CE15A, and *Cu*GE showed enzyme interactions with lignin and carbohydrate components of hardwood xylan [38,42–43]. Whereas glucuronoyl esterases were already shown to increase the hydrolytic activity of a commercial enzyme cocktail on milled corn cob [39] and endo-xylanase activity on LCCs from birchwood [40], the impact of glucuronoyl esterases on other accessory enzymes targeting xylan substitutions has not been reported.

Herein, the deconstruction of LCCs from birchwood was investigated using the family GH115 α-glucuronidases *Sde*Agu115A and *Axy*Agu115A, together with the CE15 glucuronoyl esterase *Tt*CE15A. In addition to investigating the cooperative action of these enzymes, the combined α-glucuronidase and glucuronoyl esterase treatment could be used to quantify the fraction of MeGlc*p*A in birchwood xylan extracts that participate in ester linkages to lignin.

Materials and methods

Substrates

Beechwood xylan and the K-URONIC Acid Kit were purchased from Megazyme (Bray, Ireland), D-glucuronic acid methyl ester was purchased from Carbosynth (Berkshire, UK), and 4-*O*-methyl-glucuronic acid (MeGlc*p*A) was purchased from Synthose (Concord, Canada). Organosolv hardwood lignin was provided as a gift from M. Nejad (MSU, USA). Hydrothermally extracted LCCs, fractionated into F1 and F2 fractions, were isolated from birchwood chips (*B. pendula*) as described previously [16], and received as a gift from M. Lawoko (KTH, Sweden). Briefly, ball-milled acetone-extracted birchwood was subjected to hydrothermal treatment using deionized water at 80 °C for 4 h; the supernatant component was then fractionated using a polyaromatic resin (Amberlite XAD4) into F1 and F2 fractions and lyophilized [44]. Both F1 and F2 fractions contain acetylated xylan, with Xyl*p* representing > 75% of total sugar in the fraction [16]. In the F1 fraction, 14% of Xyl*p* are acetylated at the *O*-2 position and 22% of Xyl*p* are acetylated at the *O*-3 position; in the F2 fraction, 5% of Xyl*p* are acetylated at the *O*-2 position and 7% of Xyl*p* are acetylated at the *O*-3 position [16]. Arabinose, galactose, glucose, and mannose represent less than 20% of the total sugar in both LCC fractions, and lignin comprises 4% and 6% of F1 and F2 fractions, respectively [16].

Whereas the F1 fraction was fully soluble in water, the F2 fraction was used as a stable suspension. Given the complete water solubility of the F1 fraction, it was used for both enzyme activity assays and enzyme adsorption assays, whereas the F2 fraction was used only for enzyme adsorption assays.

Quantification of MeGlc*p*A in lignin–carbohydrate complexes recovered from birchwood

A previously detailed methanolysis protocol was followed to quantify the MeGlc*p*A content in the F1 LCC fraction [45]. Briefly, 15 mg of LCCs was dried at 80 °C and then treated with 1 mL of 2 M hydrochloric acid (in anhydrous methanol) for 4 h at 100 °C. Samples were subsequently neutralized using 1 mL of 13.5 M pyridine and dried under airflow at room temperature. Dried samples were treated with 1 mL of 2 M trifluoroacetic acid at 121 °C for 1 h, after which the sample was dried under airflow at room temperature and suspended in 1 mL of de-ionized water. The amount of MeGlc*p*A released was quantified by high-performance anion-exchange chromatography (HPAEC) with pulsed amperometric detection (PAD) equipped with a CarboPac PA1 (2 × 250 mm) analytical column and corresponding guard column (2 × 50 mm) (Dionex, Sunnyvale, CA, USA). Briefly, 12.5 µL of sample was injected onto the column and eluted at 0.25 mL·min^{-1} using a gradient elution of sodium acetate, specifically 0–0.1 M sodium acetate over 35 min, followed by 0.1–0.2 M sodium acetate over 10 min, then 0.2–0.5 M sodium acetate over 5 min, and finally 0.5–0 M sodium acetate over 10 min to recondition the column. MeGlc*p*A eluted at an approximate retention time of 25 min. Data were analyzed using CHROMELEON software (version 7.2; Dionex).

Protein production

Glucuronoyl esterase from *T. turnerae* (*Tt*CE15A; PDB: 6HSW; 49 kDa) was produced as described by Arnling Bååth *et al.* [38]. Briefly, *Tt*CE15A, comprising an N-terminal His_6 tag, was expressed in *Escherichia coli* BL21 (λDE3) and purified using a 5-mL HisTrap™ Excel column. Xylan-active α-glucuronidases from *S. degradans* (*Sde*Agu115A; PDB: 4ZMH; 110 kDa) and *A. xylanus* (*Axy*Agu115A; PDB: 6PNS; GenBank: BAM48432.1, 110 kDa) were produced as described previously [24,25]. Similar to *Tt*CE15A, both *Sde*Agu115A and *Axy*Agu115A comprised His_6 tags, were expressed in *E. coli* BL21 (λDE3), and purified using Ni-NTA resin. Cells were sonicated in 50 mM HEPES pH 7.0 binding buffer containing 5% glycerol, 5 mM imidazole, and 300 mM NaCl. The supernatant was then incubated with Ni-NTA resin for 6 h at 4 °C on a vertical tube rotator at 8 r.p.m. After applying the protein sample to a column, the protein was washed with 50 mM HEPES (pH 7.0) containing 5% glycerol, 5 mM imidazole, and 300 mM NaCl. The protein was eluted using 50 mM HEPES (pH 7.0) containing 5% glycerol, 250 mM imidazole, and 300 mM NaCl. A Bio-Gel P10 column was used to exchange the protein into 50 mM HEPES buffer (pH 7.0).

Enzymatic activity toward LCCs

*Tt*CE15A, *Axy*Agu115A, and *Sde*Agu115A were tested alone and as combinations of both enzyme classes. Single enzyme reactions comprised 0.5% (w/v) LCCs in 25 mM Britton–Robinson buffer (pH 7.0) with 1 µM of each enzyme (i.e., 7.35 µg of *Tt*CE15A, 16.5 µg of *Axy*Agu115A, and 16.5 µg of *Sde*Agu115A). Reactions containing both enzyme types were set up in the same way, except they contained 1 µM *Tt*CE15A plus 1 µM α-glucuronidase, or 10 µM *Tt*CE15A plus 1 µM α-glucuronidase. The latter condition was included to investigate whether rapid separation of carbohydrates and lignin in LCCs is detrimental to the activity of α-glucuronidases due to the exposed lignin. In all cases, the final reaction volume was 150 µL. Reactions proceeded for 72 h at 25 °C in an orbital shaker at 700 r.p.m. with reaction aliquots taken at 6 and 24 h. The samples were then boiled for 6 min to stop further reactions. The earliest time point (6 h) was chosen based on preliminary assays using *Axy*Agu115A and *Sde*Agu115A to treat LCCs, where release of MeGlc*p*A was not observed by HPAEC until 4 h had elapsed [46]. Reaction supernatants were separated by centrifugation at 20 000 ***g*** for 5 min and filtered using 0.22-µm filter. The released MeGlc*p*A was then quantified using HPAEC-PAD as described above. The released lignin was followed by HPLC-UV at 210 nm (Thermo Scientific, Waltham, MA, USA, ICS 5000) equipped with an Aminex HPX87H Column (Bio-Rad, Hercules, CA, USA). For HPLC-UV, the Aminex column was equilibrated in 5 mM H_2SO_4 and conditioned to 50 °C before 12.5 µL of sample was injected onto the column and eluted at a 0.40 mL·min^{-1} using an isocratic elution of 5 mM H_2SO_4. Chromeleon software was used to analyze the obtained chromatograms.

Protein adsorption to LCCs and residual activity

To investigate adsorption of tested enzymes to F1 and F2 LCC fractions, each LCC fraction was suspended in 25 mM Britton–Robinson buffer (pH 7.0) to 1% (w/v) and then incubated with 2 µM *Tt*CE15A, *Axy*Agu115A, or *Sde*Agu115A. Enzyme binding to organosolv hardwood lignin and beechwood xylan (2% w/v, pH 7.0) was also evaluated for comparison. After incubation for 24 h at 25 °C with shaking at 700 r.p.m., samples were centrifuged (20 000 ***g***) for 5 min, and the supernatant was filtered through a 0.22-µm filter. Protein content in filtered supernatants was

quantified by gel densitometry where protein band intensities on a 10% polyacrylamide gel were determined using IMAGEJ [47] or the Bradford protein assay. Protein in the precipitate was evaluated using a PerkinElmer Paragon 500 Fourier transform infrared spectrometer in attenuated total reflectance mode (FTIR-ATR, Waltham, MA, USA). Samples were analyzed in a frequency range between 650 and 2000 cm^{-1} and at a resolution of 4 cm^{-1} with 32 scans. Spectra were visualized using SPECTRAGRYPH software (version 1.2.12, Oberstdorf, Germany).

Results and Discussion

Influence of *Tt*CE15A on α-glucuronidase activity toward isolated LCCs

The xylan-rich (F1) LCC fraction used in this study was previously extracted from birchwood and characterized in detail [16]. Similar to the previously reported 7.2 μg MeGlc*p*A per mg of the F1 LCC fraction [16], acid methanolysis of the F1 fraction performed herein confirmed 9.3 μg MeGlc*p*A per mg of sample and a MeGlc*p*A to Xyl*p* mole ratio of approximately 1 : 8.

Treatment of the F1 LCC fraction with either *Axy*Agu115A or *Sde*Agu115A released 20 ± 2% and 22.5 ± 0.8%, respectively, of total MeGlc*p*A after 6 h, and 29 ± 2% and 26.9 ± 0.1%, respectively, of total MeGlc*p*A after 24 h (Fig. 1). After 72 h, the extent of MeGlc*p*A released by *Axy*Agu115A and *Sde*Agu115A had increased to 60 ± 1% and 51.5 ± 0.8%, respectively (Fig. 1). Treatment of the F1 LCC fraction with *Tt*CE15A did not lead to release MeGlc*p*A from the substrate, consistent with all MeGlc*p*A units in the sample being bound to xylan. Instead, adding equimolar *Tt*CE15A to reactions containing *Axy*Agu115A led to release of 35 ± 1%, 68 ± 3%, and 94 ± 4% of total MeGlc*p*A after 6, 24, and 72 h, respectively. This corresponds to an increase in MeGlc*p*A release of approximately 34% after 72 h, compared to treatments with *Axy*Agu115A alone. Comparing the reactions containing *Axy*Agu115A with and without *Tt*CE15A supports the conclusion that 34–40% of MeGlc*p*A present in the LCC substrate is linked to lignin, which is in agreement with the reported amount of xylan that participates in ester linkages in beechwood LCCs [18,19]. Similarly, the addition of *Tt*CE15A increased MeGlc*p*A release by *Sde*Agu115A after 6 and 24 h to 31.6 ± 0.2% and 64.0 ± 0.8%, respectively; however, in this case, incubation up to 72 h did not substantially increase these values (66.5 ± 13%) (Fig. 1). *Tt*CE15A was thus able to boost the action of both α-glucuronidases, though the effect was less pronounced for *Sde*Agu115A than for *Axy*Agu115A. The comparatively low impact of *Tt*CE15A on *Sde*Agu115A performance is consistent with the generally poorer performance of *Sde*Agu115A compared with *Axy*Agu115A [25]. For instance, the different impacts of *Tt*CE15A on *Axy*Agu115A and *Sde*Agu115A performance might be attributed to remaining substitutions on the xylan backbone (e.g., acetyl groups), or relative positioning of MeGlc*p*A substituents that could influence *Sde*Agu115A activity.

In addition to underscoring differences in *Axy*Agu115A and *Sde*Agu115A performance, the current analyses shed light on the composition of the LCC substrate. In an earlier study, we showed the beneficial impact of the acetyl xylan esterase from *Flavobacterium johnsoniae*, *Fj*AcXE, on MeGlc*p*A release by *Axy*Agu115A from (2-*O*-MeGlc*p*A)3-*O*-acetyl-Xyl*p*

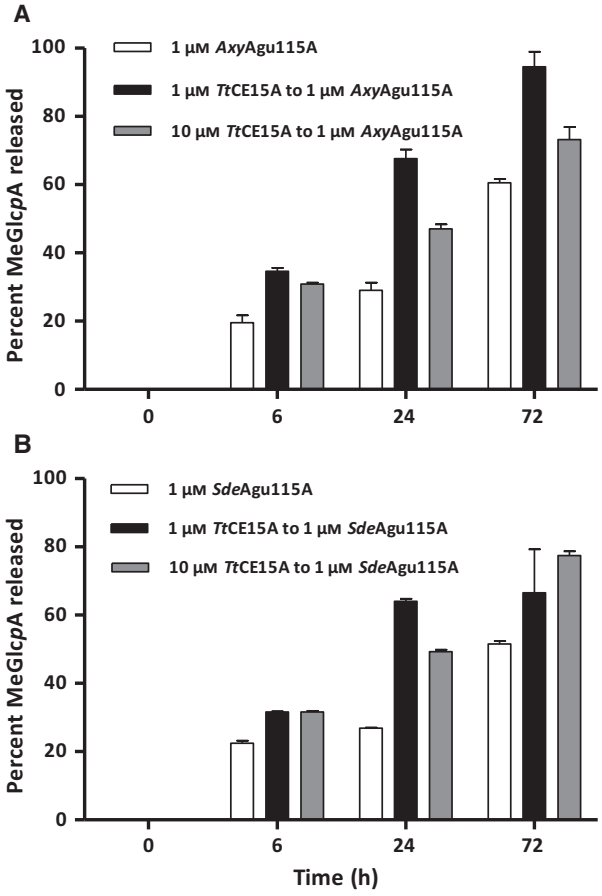

Fig. 1. Release of MeGlc*p*A from birchwood LCC (fraction F1) [16] using (A) 1 μM (110 ng·μL^{-1}) *Axy*Agu115A (white bars) with and without 1 μM (50 ng·μL^{-1}) *Tt*CE15A (black bars) or 10 μM (500 ng·μL^{-1}) *Tt*CE15A (gray bars), and (B) 1 μM (110 ng·μL^{-1}) *Sde*Agu115A (white bars) with and without 1 μM (50 ng·μL^{-1}) *Tt*CE15A (black bars) or 10 μM (500 ng·μL^{-1}) *Tt*CE15A (gray bars). Error bars represent SD (n = 2).

positions in acetylated 4-*O*-(methyl)glucuronoxylans [29]. More recently, we confirmed that *Axy*Agu115A was able to release > 98% of MeGlc*p*A present in extensively deacetylated xylan from hardwood [46]. The LCCs used in the present study have previously been analyzed by 2D HSQC NMR, which confirmed partial acetylation at *O*-2 and *O*-3 positions of Xyl*p* residues [16]. Accordingly, when considering these earlier findings together with the observation herein that over 94% of available MeGlc*p*A in the F1 LCC fraction is released by the combined action of *Tt*CE15A on *Axy*Agu115A, we can conclude that most acetylated Xyl*p* residues in the LCC fraction do not also carry esterified MeGlc*p*A.

Influence of *Axy*Agu115A on *Tt*CE15A activity toward isolated LCCs

Enzymatic release of carbohydrates from LCCs is expected to decrease lignin solubility due to increased hydrophobicity; accordingly, HPLC-UV can be used to follow changes in the soluble lignin content of the F1 LCC after treatment with *Tt*CE15, *Axy*Agu115A, and the combined enzyme reactions (Fig. 2). Notably, since *Sde*Agu115A was less active than *Axy*Agu115A, *Sde*Agu115A was not included in these experiments.

The UV absorbance of reaction supernatants containing the F1 LCC decreased by 60% after treatment for 6 h with *Tt*CE15A. This value was not significantly impacted in reactions additionally containing *Axy*Agu115A. These results support the prediction that xylans do not hinder glucuronoyl esterase access to target linkages [42,43], and indicate that glucuronoyl esterases likely act before α-glucuronidases and do not merely release single MeGlc*p*A residues linked to lignin that remain after α-glucuronidase action. This observation is also supported by crystal structures of GEs with bound MeGlc*p*A-appended xylo-oligosaccharide ligands [42,43].

Selective adsorption of α-glucuronidases to LCC-derived precipitates

Increasing the concentration of *Tt*CE15A tenfold decreased the extent of MeGlc*p*A released from F1 LCC in reactions containing *Axy*Agu115A (Fig. 1) and led to the formation of an observable precipitate. FTIR analysis of the precipitate revealed signature amide I (1650 cm^{-1}) and amide II (1550 cm^{-1}) vibrations [48] (Fig. 3), consistent with the presence of protein. Notably, characteristic vibrations for xylan and lignin were not detected in these samples. Given that the protein precipitate only formed in the presence of the LCC substrate, it is conceivable that the amended enzymes adsorbed to the surface of the LCC components, thereby masking corresponding xylan and lignin signals.

To investigate possible preferential binding of the tested enzymes to the LCCs, *Tt*CE15A, *Axy*Agu115A,

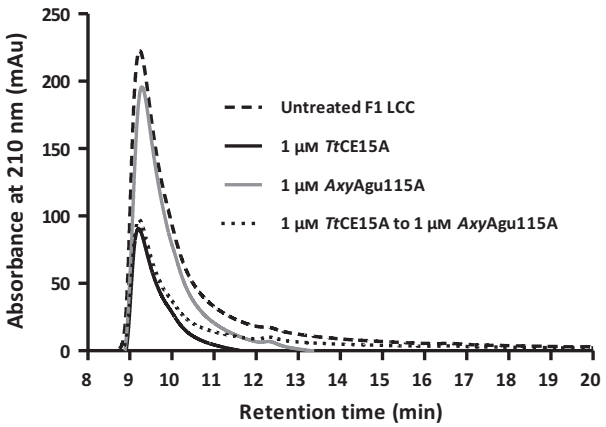

Fig. 2. HPLC-UV analysis of sample supernatants prepared from birchwood LCC (fraction F1) [16] before (dashed black line) and after 6 h treatment with 1 μM (50 ng·μL^{-1}) *Tt*CE15A (solid black line), 1 μM (110 ng·μL^{-1}) *Axy*Agu115A (solid gray line), or 1 μM (50 ng·μL^{-1}) *Tt*CE15A and 1 μM (110 ng·μL^{-1}) *Axy*Agu115A (dotted line).

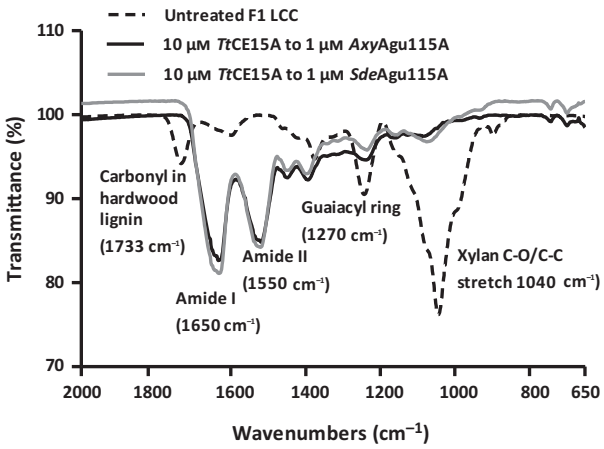

Fig. 3. FTIR spectra of birchwood LCC (fraction F1) [16] before (dashed black line) and after treatment with 10 μM (500 ng·μL^{-1}) *Tt*CE15A and 1 μM (110 ng·μL^{-1}) *Axy*Agu115A (solid black line), or 10 μM (500 ng·μL^{-1}) *Tt*CE15A and 1 μM (110 ng·μL^{-1}) *Sde*Agu115A (solid gray line). After enzyme treatment, the resulting precipitates lack the xylan signal at wavenumber 1040 cm^{-1} [50] and lignin signals at 1733 and 1270 cm^{-1} [51], and gain signals at wavenumber 1550 and 1650 cm^{-1}, indicating adsorbed protein [48].

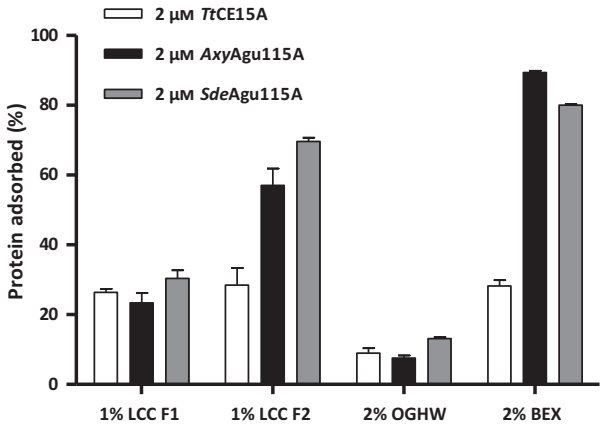

Fig. 4. Adsorption of enzymes to birchwood LCC (fractions F1 and F2) [16], organosolv hardwood lignin (OGHW), and beechwood glucuronoxylan (BEX). Percent of protein adsorbed to LCC F1 (Fig. S1) and BEX were evaluated using gel densitometry (Fig. S2), while LCC F2 and OGHW were evaluated using the Bradford protein assay. Error bars represent SD ($n = 2$).

and *Sde*Agu115A were each tested for adsorption to F1 and F2 LCC fractions, where the F2 fraction is distinguished by lower water solubility and higher lignin content (i.e., 4% lignin in F1 and 6% lignin in F2) [15]. While the enzymes adsorbed to the F1 LCC fraction to similar extents (23–30% of total protein; Fig. 4), both α-glucuronidases displayed two times higher adsorption to the F2 LCC fraction (57–70% of total protein; Fig. 4). Notably, all tested enzymes bound organosolv lignin to similar extents (< 15%); by contrast, the amount of *Axy*Agu115A and *Sde*Agu115A bound to glucuronoxylan was approximately three times higher than that measured for *Tt*CE15A (Fig. 4). The comparatively low adsorption of *Tt*CE15A to the F2 LCC fraction, as well as organosolv lignin and glucuronoxylan, might be attributed to the necessary functional association of glucuronoyl esterases with diverse lignin–carbohydrate structures.

Conclusions

This study confirmed the activities of the glucuronoyl esterase *Tt*CE15A and two α-glucuronidases in disassembly of LCCs isolated from birchwood. In particular, the release of MeGlc*p*A by *Axy*Agu115A improved significantly in combination with *Tt*CE15A, and monitoring the reaction after indicated that 34% of MeGlc*p*A in the birchwood LCC sample was ester-linked to lignin. It is conceivable that the release of xylan from LCCs is responsible for the reduction in soluble enzyme concentrations in our reactions. Supplementing reactions with known additives that reduce nonproductive associations with lignin (e.g., addition of surfactant or BSA) could possibly curtail this effect, while the addition of xylan-degrading enzymes may reduce the adsorption of α-glucuronidases to precipitated xylan. The combination of α-glucuronidase and glucuronoyl esterase activities on LCCs confirmed through this study sets a precedence of using such enzyme systems for xylan recovery and substrate characterization, and thus motivates the search for new α-glucuronidases and glucuronoyl esterases with faster release of MeGlc*p*A.

Acknowledgements

The authors thank Dr Nicola Giummarella, Assoc Prof Martin Lawoko, and Assoc Prof Francisco Javier Vilaplana Domingo for providing LCCs used in preliminary studies, and Prof Mojgan Nejad for providing organosolv lignin. ERM thanks Genome Canada for the project 'SYNBIOMICS – Functional genomics and techno-economic models for advanced biopolymer synthesis' (LSARP, Grant No. 10405) and the European Research Council (ERC) Consolidator Grant to ERM (BHIVE—648925) for funding. LO, JL, and JAB thank Knut and Alice Wallenberg Foundation for funding (Wallenberg Wood Science Center). JAB thanks Gunnar Sundblad Research Foundation for the stipend, making the trip to Toronto possible.

Author contributions

ERM, JL, and LO conceived the study; ERM and LO supervised the study; OR, JAB, and TVV designed experiments; OR and JAB performed experiments; OR and TVV analyzed data; OR and ERM wrote the manuscript; and OR, JAB, TVV, JL, ERM, and LO made manuscript revisions.

Data accessibility

Research data pertaining to this article are located at figshare.com: https://doi.org/10.6084/m9.figshare.13547270.v1.

References

1 Jacobs A, Larsson PT and Dahlman O (2001) Distribution of uronic acids in xylans from various species of soft- and hardwood as determined by MALDI mass spectrometry. *Biomacromol* **2**, 979–990.
2 Teleman A, Tenkanen M, Jacobs A and Dahlman O (2002) Characterization of O-acetyl-(4-O-

methylglucurono)xylan isolated from birch and beech. *Carbohyd Res* **337**, 373–377.
3 Kabel MA, De Waard P, Schols HA and Voragen AGJ (2003) Location of O-acetyl substituents in xylo-oligosaccharides obtained from hydrothermally treated Eucalyptus wood. *Carbohyd Res* **338**, 69–77.
4 Escalante A, Gonçalves A, Bodin A, Stepan A, Sandström C, Toriz G and Gatenholm P (2012) Flexible oxygen barrier films from spruce xylan. *Carbohyd Polym* **87**, 2381–2387.
5 Busse-Wicher M, Grantham NJ, Lyczakowski JJ, Nikolovski N and Dupree P (2016) Xylan decoration patterns and the plant secondary cell wall molecular architecture. *Biochem Soc Trans* **44**, 74.
6 Grantham NJ, Wurman-Rodrich J, Terrett OM, Lyczakowski JJ, Stott K, Iuga D, Simmons TJ, Durand-Tardif M, Brown SP, Dupree R *et al.* (2017) An even pattern of xylan substitution is critical for interaction with cellulose in plant cell walls. *Nat Plants* **3**, 859–865.
7 Dupree R, Simmons TJ, Mortimer JC, Patel D, Iuga D, Brown SP and Dupree P (2015) Probing the molecular architecture of *Arabidopsis thaliana* secondary cell walls using two- and three-dimensional ^{13}C solid state nuclear magnetic resonance spectroscopy. *Biochemistry* **54**, 2335–2345.
8 Simmons TJ, Mortimer JC, Bernardinelli OD, Pöppler A-C, Brown SP, Deazevedo ER, Dupree R and Dupree P (2016) Folding of xylan onto cellulose fibrils in plant cell walls revealed by solid-state NMR. *Nat Commun* **7**, 13902.
9 Terrett OM, Lyczakowski JJ, Yu L, Iuga D, Franks WT, Brown SP, Dupree R and Dupree P (2019) Molecular architecture of softwood revealed by solid-state NMR. *Nat Commun* **10**, 4978.
10 Busse-Wicher M, Gomes TCF, Tryfona T, Nikolovski N, Stott K, Grantham NJ, Bolam DN, Skaf MS and Dupree P (2014) The pattern of xylan acetylation suggests xylan may interact with cellulose microfibrils as a twofold helical screw in the secondary plant cell wall of *Arabidopsis thaliana*. *Plant J* **79**, 492.
11 Das NN, Das SC and Mukherjee AK (1984) On the ester linkage between lignin and 4-O-methyl-D-glucurono-D-xylan in jute fiber (*Corchorus capsularis*). *Carbohyd Res* **127**, 345–348.
12 Martínez-Abad A, Berglund J, Toriz G, Gatenholm P, Henriksson G, Lindström M, Wohlert J and Vilaplana F (2017) Regular motifs in xylan modulate molecular flexibility and interactions with cellulose surfaces. *Plant Physiol* **175**, 1579–1592.
13 Arnling Bååth J, Giummarella N, Klaubauf S, Lawoko M and Olsson L (2016) A glucuronoyl esterase from *Acremonium alcalophilum* cleaves native lignin-carbohydrate ester bonds. *FEBS Lett* **590**, 2611–2618.
14 Balakshin M, Capanema E and Berlin A (2014) Isolation and analysis of lignin–carbohydrate complexes preparations with traditional and advanced methods: a review. In Studies in Natural Products Chemistry (Atta-ur-Rahman F, ed.), pp. 83–115. Elsevier, Amsterdam.
15 Balakshin MY, Capanema EA and Chang HM (2007) MWL fraction with a high concentration of lignin-carbohydrate linkages: isolation and 2D NMR spectroscopic analysis. *Holzforschung* **61**, 1–7.
16 Giummarella N and Lawoko M (2016) Structural basis for the formation and regulation of lignin–xylan bonds in birch. *ACS Sustain Chem Eng* **4**, 5319–5326.
17 Jeffries TW (1991) Biodegradation of lignin-carbohydrate complexes. In Physiology of Biodegradative Microorganisms (Ratledge C ed.), pp. 163–176. Springer Netherlands, Dordrecht.
18 Imamura T, Watanabe T, Kuwahara M and Koshijima T (1994) Ester linkages between lignin and glucuronic acid in lignin-carbohydrate complexes from *Fagus crenata*. *Phytochemistry* **37**, 1165–1173.
19 Takahashi N and Koshijima T (1988) Ester linkages between lignin and glucuronoxylan in a lignin-carbohydrate complex from beech (*Fagus crenata*) wood. *Wood Sci Technol* **22**, 231–241.
20 Álvarez C, Reyes-Sosa FM and Díez B (2016) Enzymatic hydrolysis of biomass from wood. *Microb Biotechnol* **9**, 149–156.
21 Bhattacharya AS, Bhattacharya A and Pletschke BI (2015) Synergism of fungal and bacterial cellulases and hemicellulases: a novel perspective for enhanced bio-ethanol production. *Biotech Lett* **37**, 1117–1129.
22 de Vries RP, Kester HC, Poulsen CH, Benen JA and Visser J (2000) Synergy between enzymes from *Aspergillus* involved in the degradation of plant cell wall polysaccharides. *Carbohyd Res* **327**, 401–410.
23 Mckee LS, Sunner H, Anasontzis GE, Toriz G, Gatenholm P, Bulone V, Vilaplana F and Olsson L (2016) A GH115 α-glucuronidase from *Schizophyllum commune* contributes to the synergistic enzymatic deconstruction of softwood glucuronoarabinoxylan. *Biotechnol Biofuels* **9**, 2.
24 Wang W, Yan R, Nocek BP, Vuong TV, Di Leo R, Xu X, Cui H, Gatenholm P, Toriz G, Tenkanen M *et al.* (2016) Biochemical and structural characterization of a five-domain GH115 α-glucuronidase from the marine bacterium *Saccharophagus degradans* 2–40^T. *J Biol Chem* **291**, 14120–14133.
25 Yan R, Vuong TV, Wang W and Master ER (2017) Action of a GH115 α-glucuronidase from *Amphibacillus xylanus* at alkaline condition promotes release of 4-O-methylglucopyranosyluronic acid from glucuronoxylan and arabinoglucuronoxylan. *Enzyme Microb Technol* **104**, 22–28.

26 Spanikova S and Biely P (2006) Glucuronoyl esterase – novel carbohydrate esterase produced by *Schizophyllum commune*. *FEBS Lett* **580**, 4597–4601.

27 D'errico C, Jørgensen JO, Krogh KBRM, Spodsberg N, Madsen R and Monrad RN (2015) Enzymatic degradation of lignin-carbohydrate complexes (LCCs): Model studies using a fungal glucuronoyl esterase from *Cerrena unicolor*. *Biotechnol Bioeng* **112**, 914–922.

28 De Santi C, Gani OA, Helland R and Williamson A (2017) Structural insight into a CE15 esterase from the marine bacterial metagenome. *Sci Rep* **7**, 17278.

29 Razeq FM, Jurak E, Stogios PJ, Yan R, Tenkanen M, Kabel MA, Wang W and Master ER (2018) A novel acetyl xylan esterase enabling complete deacetylation of substituted xylans. *Biotechnol Biofuels* **11**, 74.

30 Wang W, Mai-Gisondi G, Stogios PJ, Kaur A, Xu X, Cui H, Turunen O, Savchenko A and Master ER (2014) Elucidation of the molecular basis for arabinoxylan-debranching activity of a thermostable family GH62 α-L-arabinofuranosidase from *Streptomyces thermoviolaceus*. *Appl Environ Microbiol* **80**, 5317–5329.

31 Aalbers F, Turkenburg JP, Davies GJ, Dijkhuizen L and Lammerts Van Bueren A (2015) Structural and functional characterization of a novel family GH115 4-O-methyl-α-glucuronidase with specificity for decorated arabinogalactans. *J Mol Biol* **427**, 3935–3946.

32 Rogowski A, Baslé A, Farinas CS, Solovyova A, Mortimer JC, Dupree P, Gilbert HJ and Bolam DN (2014) Evidence that GH115 α-glucuronidase activity, which is required to degrade plant biomass, is dependent on conformational flexibility. *J Biol Chem* **289**, 53–64.

33 Rhee MS, Sawhney N, Kim YS, Rhee HJ, Hurlbert JC, St. John FJ, Rice JD and Preston JF (2017) GH115 α-glucuronidase and GH11 xylanase from *Paenibacillus* sp. JDR-2: potential roles in processing glucuronoxylans. *Appl Microbiol Biotechnol* **101**, 1465–1476.

34 Martínez PM, Appeldoorn MM, Gruppen H and Kabel MA (2016) The two *Rasamsonia emersonii* α-glucuronidases, ReGH67 and ReGH115, show a different mode-of-action towards glucuronoxylan and glucuronoxylo-oligosaccharides. *Biotechnol Biofuels* **9**, 105.

35 Fujimoto Z, Ichinose H, Biely P and Kaneko S (2011) Crystallization and preliminary crystallographic analysis of the glycoside hydrolase family 115 α-glucuronidase from *Streptomyces pristinaespiralis*. *Acta Crystallogr Sect F Struct Biol Cryst Commun* **67** (Pt 1), 68–71.

36 Bajwa PK, Harrington S, Dashtban M and Lee H (2016) Expression and characterization of glycosyl hydrolase family 115 α-glucuronidase from *Scheffersomyces stipitis*. *Ind Biotechnol* **12**, 98–104.

37 Ryabova O, Vršanská M, Kaneko S, Van Zyl WH and Biely P (2009) A novel family of hemicellulolytic α-glucuronidase. *FEBS Lett* **583**, 1457–1462.

38 Arnling Bååth J, Mazurkewich S, Navarro Poulsen J-C, Olsson L, Leggio LL and Larsbrink J (2019) Structure-function analyses reveal that a glucuronoyl esterase from *Teredinibacter turnerae* interacts with carbohydrates and aromatic compounds. *J Biol Chem* **294**, 6635–6644.

39 Arnling Bååth J, Mazurkewich S, Knudsen RM, Poulsen J-CN, Olsson L, Lo Leggio L and Larsbrink J (2018) Biochemical and structural features of diverse bacterial glucuronoyl esterases facilitating recalcitrant biomass conversion. *Biotechnol Biofuels* **11**, 213.

40 Mosbech C, Holck J, Meyer AS and Agger JW (2018) The natural catalytic function of cuge glucuronoyl esterase in hydrolysis of genuine lignin-carbohydrate complexes from birch. *Biotechnol Biofuels* **11**, 1–9.

41 Mosbech C, Holck J, Meyer AS and Agger JW (2019) Enzyme kinetics of fungal glucuronoyl esterases on natural lignin-carbohydrate complexes. *Appl Microbiol Biotechnol*. **103**, 4065–4075.

42 Mazurkewich S, Poulsen J-CN, Lo Leggio L and Larsbrink J (2019) Structural and biochemical studies of the glucuronoyl esterase *Ot*CE15A illuminate its interaction with lignocellulosic components. *J Biol Chem*. **294**, 19978–19987.

43 Ernst HA, Mosbech C, Langkilde AE, Westh P, Meyer AS, Agger JW and Larsen S (2020) The structural basis of fungal glucuronoyl esterase activity on natural substrates. *Nat Commun* **11**, 1026.

44 Schwartz TJ and Lawoko M (2010) Removal of acid-soluble lignin from biomass extracts using Amberlite Xad-4 resin. *BioResources* **5**, 2337–2347.

45 Morais De Carvalho D, Martínez-Abad A, Evtuguin DV, Colodette JL, Lindström ME, Vilaplana F and Sevastyanova O (2017) Isolation and characterization of acetylated glucuronoarabinoxylan from sugarcane bagasse and straw. *Carbohyd Polym* **156**, 223–234.

46 Vuong TV and Master ER (2020) Enzymatic production of 4-O-methyl D-glucaric acid from hardwood xylan. *Biotechnol Biofuels* **13**, 51.

47 Schneider CA, Rasband WS and Eliceiri KW (2012) NIH image to imageJ: 25 years of image analysis. *Nat Methods* **9**, 671–675.

48 Chittur KK (1998) FTIR/ATR for protein adsorption to biomaterial surfaces. *Biomaterials* **19**, 357–369.

49 Eriksson T, Börjesson J and Tjerneld F (2002) Mechanism of surfactant effect in enzymatic hydrolysis of lignocellulose. *Enzyme Microb Technol* **31**, 353–364.

50 Coimbra MA, Barros A, Rutledge DN and Delgadillo I (1999) FTIR spectroscopy as a tool for the analysis of olive pulp cell-wall polysaccharide extracts. *Carbohyd Res* **317**, 145–154.

51 Faix O (1991) Classification of lignins from different botanical origins by FTIR spectroscopy. *Holzforschung* **45** (s1), 21.

Supporting information

Additional supporting information may be found online in the Supporting Information section at the end of the article.

Table S1. Substrate preference of GH115 α-glucuronidases based on relative release of MeGlcpA.

Fig S1. Gel densitometry of reaction supernatant for evaluating adsorption of enzymes to birchwood LCC F1 [16].

Fig S2. Gel densitometry of reaction supernatant for evaluating adsorption of enzymes to beechwood glucuronoxylan.